CHAPTER

23 Experimental and numerical models of fine sediment transport by tsunamis

Davin J. Wallace[1], **Jonathan D. Woodruff**[2]

[1]*School of Ocean Science and Engineering, University of Southern Mississippi, Stennis Space Center, MS, United States;* [2]*Department of Geosciences, University of Massachusetts Amherst, Amherst, MA, United States*

Abstract

Tsunamis and storms can be incredibly destructive events. The direct observational record of important characteristics of these events, such as flooding height, inundation, and flow speed, is often lacking. Coupled with field data acquisition, a tremendous amount of additional information can be gained through experimental laboratory studies and by applying numerical inverse models to mud and sand deposits often associated with these events. This chapter outlines typical field and sampling approaches to study tsunami-derived deposits, common data modeling techniques for constraining/reconstructing flood conditions from resultant deposits, experimental investigations, and future directions in the field.

Keywords: Event deposits; Experimental model; Inverse model; Numerical model; Sediment transport; Storm; Tsunami.

Introduction

Tsunamis and storms are often devastating events that can cause tremendous loss of life and financial cost. The largest and most destructive events are rare, meaning that data from them are limited to sparse direct observations during the abridged historical record. Even with modern technology, it is still challenging to fully capture and observe sediment transport patterns associated with tsunami and storm events. Experimental and numerical models of fine sediment (defined in this chapter as mud to sand) transport offer very important constraints that provide a unique opportunity to understand these events in greater detail. In many instances, experiments/models that are applicable to modern and ancient events serve as the only available tool to constrain flood and flow magnitudes and gain a better understanding of the process of tsunami inundation. By incorporating field-based information and making appropriate assumptions about a particular event, inverse numerical models allow important tsunami characteristics to be calculated and/or constrained. Experimental

Geological Records of Tsunamis and Other Extreme Waves. https://doi.org/10.1016/B978-0-12-815686-5.00023-7

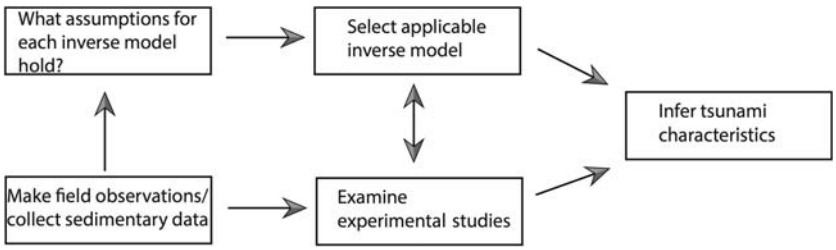

FIGURE 23.1

Flow chart summarizing this chapter.

(or laboratory flume) studies examine tsunami and storm impacts in a controlled environment, often shedding light on hydrodynamic conditions and the resulting sedimentary deposits. All three techniques together can be viewed as a holistic approach (Fig. 23.1). Ultimately, this information provides an important context that can be used for coastal planning of disaster mitigation activities, such as designing and implementing coastal engineering structures, producing evacuation and geohazard maps, and making management decisions.

Tsunamis and storms have the ability to move sediment of all sizes ranging from mud all the way to megaboulders. The depositional patterns (Chapter 11) in tsunami deposits preserved within the geological record have been studied for decades (e.g., Shepard et al., 1950; Kon'no, 1961; Coleman, 1968; Makino, 1968). Modern storm overwash has also been extensively studied (e.g., Hayes, 1967; Morton, 1979; Nummedal et al., 1980; Kahn and Roberts, 1982; Stone and Wang, 1999; Donnelly et al., 2006; La Selle et al., 2017). Much can be learned from the resultant sedimentary deposits left behind from these events, where fine-grained deposition (i.e., mud to sand sizes) is often a defining feature. A landward thinning and fining of the deposit is generally observed in tsunami deposits (Fig. 23.2), with a sharp, often erosive bottom contact containing rip-up clasts (Sugawara et al., 2014). The presence of marine diatoms and foraminifera within the deposit can indicate a marine source (Chapter 12; Chapter 14; Pilarczyk et al., 2014). The deposit geometry is a feature that may be useful for discrimination between tsunami and storm deposits (Morton et al., 2007). Sedimentary structures within flood deposits are often useful to elucidate physical processes. For example, tsunami deposits often contain larger distinct units of fining upward sequences from suspension deposition (Jaffe et al., 2012). Storm overwash stratigraphy is in general a result of a larger number of shorter wind waves that can lead to complex, fine-scale depositional strata often truncated by erosional surfaces. However, there is no robust criterion for unequivocally delineating tsunami and storm deposits as they can consist of similar structures (Switzer and Jones, 2008).

Coupling or comparing this sedimentary information with experimental models and more detailed numerical simulations constitutes a powerful tool to explore characteristics of tsunami events (Fig. 23.1), which are challenging or impossible to measure otherwise. This includes important tsunami parameters such as inundation area, speed, runup height, and flow depth. Direct instrumental and video

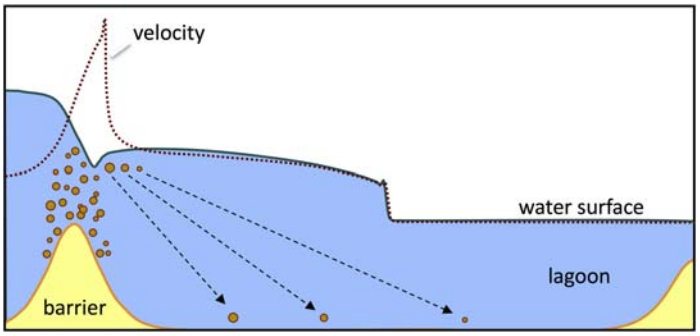

FIGURE 23.2

Schematic of tsunami wave overwashing a barrier beach and inundating a back-barrier lagoon. Water surface (*blue*) and corresponding velocities (*red*) are based on simulations and highlight the high velocities and transition to near critical flow over the barrier. These high velocities also result in enhanced turbulence that serves to suspend sediment throughout the water column. Following advection into the lagoon, velocities and corresponding turbulence are reduced, which results in the settling of grains and a landward fining of the resulting deposit.

Adapted from Woodruff et al. (2008).

observations of these flood characteristics are often unavailable, and proxy estimates following the event (e.g., elevations of wrack lines and other high-water marks) are often associated with significant uncertainty. Because of the complexities and uncertainty associated with these parameters, there is great value in obtaining additional constraints via experimental studies and modeling of sediment transport, which is an intrinsically collaborative process, involving geology, hydrodynamics, hydraulics, mathematics, and physics. Inverse numerical simulations of fine sediment transport by tsunamis are separated into forward and inverse approaches. See Sugawara et al. (2014) for a discussion of the information that can be learned from forward modeling approaches. Since the focus of this chapter is primarily on initial field-based inputs to extract useful information from deposits (for example, see the information extracted from Woodruff et al. (2008) shown in Fig. 23.2), we focus our discussion on general laboratory studies and inverse approaches on tsunami deposits. Under appropriate assumptions, both types of approaches are applicable to storm events as well.

This chapter describes typical field surveys, sample methods, common calculations related to each inverse model, experimental approaches, challenges, and future directions. It is intended to be used to select field sites and sampling strategies to obtain the necessary data required for basic inverse model applications or experimental studies (Fig. 23.1). The type of inverse model used should be related to the appropriate assumptions for a given tsunami or storm scenario, as outlined subsequently (Table 23.1). This coupled information can also be helpful in experimental study setup and determining comparability.

Table 23.1 Inverse approaches, basic assumptions involved, major inputs, and major outputs.

Inverse model approach	References	Basic assumptions	Major inputs	Major outputs
Particle settling	Smith et al. (2007)	Sediment transported in suspension; sediment gradually settles out from suspension during each impacting tsunami wave producing fining upward sequences; depositional time for each sequence is related to an assumed wave period	Slowest settling velocity	Tsunami water depth
Particle trajectory	Soulsby et al. (2007)	Maximum depth of inundation decreases linearly with distance from the shoreline; suspension transport; settling treated as a moving sediment column until all sediment in the water deposited; landward thinning deposit	Settling velocities at several locations within deposit; deposit thickness measurements; grain size distributions within deposit	Runup height; inundation distance
Particle trajectory	Moore et al. (2007)	Suspension transport; no resuspension after deposition; large grain sizes fully suspended within water column; law of the wall applicable	Largest particle settling velocity (D_{90} or D_{95}); particle distance traveled	Tsunami height; spatially-averaged flow speed

Table 23.1 Inverse approaches, basic assumptions involved, major inputs, and major outputs.—*cont'd*

Inverse model approach	References	Basic assumptions	Major inputs	Major outputs
TsuSedMod: Equilibrium suspension	Jaffe and Gelfenbaum (2007)	Suspension transport; steady flow turbulence formulation applicable; significant sediment supply for suspension; equilibrium suspension; deposit components from clearing suspended sediment; no erosion/ resuspension during settling or from backwash	Settling velocities at suspension-graded sections; flow depth; bottom roughness	Shear velocity; depth-averaged and maximum velocity

Field surveys and sample analysis methods

There are many important considerations for post-event field survey and reconnaissance efforts (Chapter 10 ITST, 2014; Wilson et al., 2015). After a tsunami event occurs, it is important to access a site where field observations and measurements will take place soon after the event. Primary reasons for rapid sampling are related to the ephemeral nature of water level indicators and the fact that weathering, bioturbation, and human response efforts that often times move sediment will disturb sedimentary deposits. With respect to event deposits, post-tsunami surveys are often conducted away from developed areas to avoid human impacts and flow and transport complexities associated with manmade structures. Additionally, plants and animals can rapidly colonize and alter the sedimentary sequences through bioturbation, and natural physical post-depositional reworking can also occur via rain, wind, etc. Selecting a site with observational information can be quite advantageous for comparisons of model outputs and experimental studies. One strategy typically employed to discover potential sites and deposits is utilizing pre- and post-event aerial imagery and response surveys often conducted by government agencies.

Another important consideration for field surveys and sample locations concerns the environment targeted. Typical environments have a prominent source of material (i.e., sediment supply) and an area with some degree of preservation potential. For paleo-studies, it is incredibly important to select a site with high long-term preservation potential. The integration of observations with models/experiments often requires elevation measurements of the coastal setting along with notes on where coastal geomorphology could have been altered significantly during the tsunami event. In general, these practices can lead to the study of natural event stratigraphy, a key component to extracting the necessary information to apply inverse models and comparability to experimental work.

Once a potential event deposit is discovered, there are a general set of best practices for information to collect and observations to make. The first step involves field mapping of the sedimentary deposit, noting the extent of deposition both horizontally and laterally. This is an important step as it allows for a quantification of the potential sediment flux (when combined with sufficient estimates of sediment dry bulk density). This could also involve runup and inundation measurements of the event, which are frequently used to inform or validate numerical models (Satake et al., 1993; Piatanesi et al., 1996; Synolakis and Okal, 2005). Sampling the deposit at a resolution that best captures the spatial variability (both vertical and horizontal) is also critical, not only to obtain subsamples for dry bulk density measurements, but also for future analyses of grain size and composition.

Trenches can be dug to sample important facies, making particular note of where the deposit transitions into the pre-event sediments. Sediment cores can also be collected in lieu of trenches. One advantage of trenches is that subtle, spatially varying sedimentary features can be identified, perhaps indicating runup versus backwash processes. One advantage of sediment cores is that in situ material can be collected and returned to the lab. Much deeper and continuous sedimentary records can also be collected with sediment cores, which often allows for the analysis of older event layer deposits preserved at a particular location. For either trenches or cores, the next steps involve targeting shore-normal and parallel transects that adequately describe the spatial distribution and variability of a particular deposit. It is difficult to recommend a single strategy of distance between samples; however, an estimate could be based on gridding the aerial extent of the deposit at a resolution that is feasible to sample in the time allotted. It is important to note that oftentimes follow-up fieldwork and data collection is necessary as no two event deposits are identical, so it can be challenging to collect all necessary data from one field campaign.

Accurate measurements of each sample location and associated elevations in the field are important for future assessments of sediment transport distance. If possible, the source of material being transported (from the beach, offshore, etc.), should be identified and sampled as well. Within the deposit, there are a number of grain size observations that should be made. First, the deposit thickness should be measured. Occasionally, it is not obvious where one deposit begins and ends, or how to delineate between event and non-event sedimentation. For paleotsunami and storm

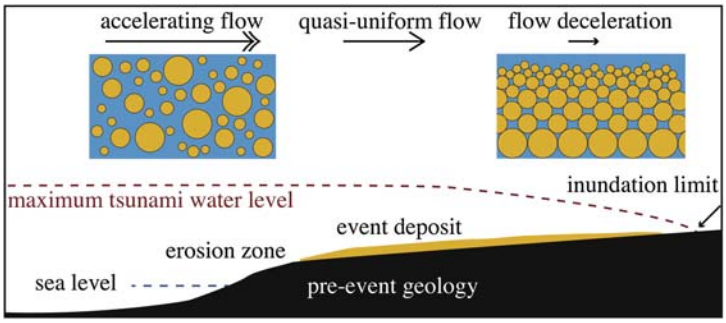

FIGURE 23.3

Schematic model of tsunami event sedimentation, depositional processes, and extent. Grains (*orange circles*) begin to settle out of suspension in a zone of spatially quasi-uniform flow and deceleration as it moves onshore (*blue boxes*). Note normal and/or suspension grading occurring in right blue inset.

Adapted from Jaffe and Gelfenbaum (2007).

investigations, it is often necessary to use a variety of dating techniques including tephra (Page et al., 2010), ^{14}C (Libby et al., 1949; Libby, 1955), ^{210}Pb (Faure, 1986), ^{137}Cs (DeLaune et al., 1978), pollen (Rich, 1970; Brugam, 1978), and industrial heavy metals (McCaffrey and Thomson, 1980; Bricker-Urso et al., 1989) to obtain a sediment core chronology to better link event deposits to the timing of flood events of interest. One should also carefully observe for evidence of normal grading (i.e., fining upward), which is often indicative of sediment settling out of suspension (Fig. 23.3). Several units of normal grading are particularly useful in identifying multiple deposits or one event with different stages of deposition associated with runup and returning flows. A lack of this type of normal bedding could indicate resuspension or predominantly bed-load transport, so all sorting patterns should be noted. Finally, a full grain size distribution of the deposit, typically collected at 1-cm vertical resolution or less, is often useful. However, the grain size sampling interval should be dictated by factors such as deposit thickness and observed variability. Grain density and shape can be important properties to collect particularly when determining provenance. These particle parameters are also sometimes used to refine calculations of settling velocity, although this velocity can also be directly measured via a settling tube in the lab using the collected sediment. Fixed volume sampling also allows for dry bulk density measurements.

Inverse modeling approaches

Inverse sedimentologic modeling as defined herein is a model that uses the data obtained from sedimentary deposits associated with a tsunami or storm event to infer characteristics of the event on the basis of the first principles of hydrodynamics and sediment transport. Here, we broadly characterize the primary types of inverse

models as particle settling, particle trajectory, equilibrium suspension, and combined. When informed with measurements from resultant deposits, these models have been used to help constrain flow speed, runup height, and inundation distance. The specific model that can be applicable to a particular tsunami or storm event should be carefully related to the necessary assumptions for model validity, outlined in detail subsequently and in Table 23.1.

Particle settling

Smith et al. (2007) use the sediment characteristics associated with a paleotsunami deposit coupled with an approximate wave period to estimate flow depth. The model assumes that sediment is transported in suspension, sediment gradually settles out from suspension during each impacting tsunami wave producing fining upward sequences, and the depositional time for each sequence is related to the wave period (Table 23.1). The reconstructed tsunami water depth is calculated by assuming a wave period set to the time of settling and then using the settling velocity (w_s) of the slowest individual settling particle to infer flood depth based on equations by Soulsby (1997):

$$w_s = v/d\left[\left(10.36^2 + 1.049D_*^3\right)^{0.5} - 10.36\right] \tag{23.1}$$

where v is the kinematic viscosity, and d is the median grain diameter. The dimensionless grain size (D_*) is represented by the following:

$$D_* = \frac{[g(s-1)]^{0.333}}{[v^2]}\, d \tag{23.2}$$

where g is acceleration due to gravity, and s is ratio of the density of sediment and water. Additional settling velocity equations (e.g., Ferguson and Church, 2004) exist outside of Eq. (23.1) presented here and could be similarly substituted. The Smith et al. (2007) model was applied to the Holocene Storegga Slide tsunami at Montrose, Scotland, to estimate maximum flow depths, though it is challenging to assess the performance as it was only applied to this paleo-deposit.

Particle trajectory

Soulsby et al. (2007) present a simple trajectory-based model of tsunami hydrodynamics and sediment dynamics that can estimate runup and inundation distance from observed sedimentary deposits. Several basic assumptions are described here, but for a more robust discussion, see Soulsby et al. (2007). The maximum depth of inundation is assumed to decrease linearly with distance from the shoreline. The wave is also assumed to consist of high amounts of suspended sediment. The settling is treated as a moving sediment column until all of the sediment in the water is deposited. The contribution of grain sizes to the tsunami deposit decreases landward and results in a landward thinning deposit. Additionally, the model assumes no

resuspension after deposition (Table 23.1). The runup of sediment (R_S) is related to the runup of water (R_w):

$$R_S = \frac{R_w}{1 + \alpha\gamma} \tag{23.3}$$

where γ is the duration of uprush divided by the duration of backwash at the shoreline, and

$$\alpha = \frac{w_s T}{H} \tag{23.4}$$

where T is total inundation time, and H is the maximum tsunami depth. Tsunami deposit thickness at the shoreline (ζ_0) can be estimated using

$$\zeta_0 = \frac{\alpha(1 + \alpha\gamma)}{1 + \alpha}\left(\frac{C_0}{\rho_B}\right)H \tag{23.5}$$

where C_0 is the suspended sediment concentration in the water column, and ρ_B is the dry bulk density of the tsunami deposit. Furthermore, the thickness ($\zeta(x)$) deposited decreasing with distance x from the shoreline can be estimated using the following:

$$\zeta(x) = \zeta_0\left(1 - \frac{x}{R_S}\right) \text{ for } x \leq R_S, \text{ and 0 for x } > R_S \tag{23.6}$$

This model has been successfully applied to the 1929 Grand Banks tsunami and the Holocene Storegga Slide tsunami (Soulsby et al., 2007). Reasonably good agreement was determined between predicted and observed runup for the 1929 event, but only an estimate can be provided for the Holocene event since it is unknown.

Moore et al. (2007) developed a particle trajectory or advective settling model based on the fact that many observed tsunami deposits fine with distance inland. As coarser particles settle faster than finer particles, their transport distances tend to be less. Thus, Moore et al. (2007) essentially relate the trajectory and distance a particle travels landward by the settling velocity and wave speed assuming a constant horizontal "advective" transport velocity (Fig. 23.2). A few assumptions are necessary for this approach, namely that large grains are fully suspended within the water column at some point near the coast followed by strict settling out of suspension landward with a steady horizontal flow (Table 23.1). No resuspension occurs during settling, and it is assumed that the deposit is not source limited, so there is a sufficient supply and distribution of grain sizes at the coast for transport. Assuming particles are mixed to the top of the water column, the time, t, it takes for these grains to settle out of suspension is related to the maximum travel time that these grains can be horizontally carried to the most landward position that they are observed:

$$\frac{H}{w_S} = t = \frac{x_L}{U} \tag{23.7}$$

where H is the shoreline tsunami height, w_S is the settling velocity, x_L is the particle horizontal distance traveled, and U is the horizontal flow speed. Typically, the distance a particle travels can be measured in the field, and settling velocity can either be estimated from theoretical work (e.g., Ferguson and Church, 2004) or measured directly in the laboratory (Syvitski et al., 1991; Woodruff et al., 2008; Hong et al., 2018). The law of the wall describes how turbulence near a boundary (or wall) is related to the flow conditions associated with this boundary. The depth-averaged law of the wall relates water depth (h) to depth-averaged flow velocity (U):

$$U = \frac{u_*}{K}\left(\ln\left(\frac{h}{z_0}\right) - 1\right) \tag{23.8}$$

where u_* is the shear velocity, K is the von Kármán constant, and z_0 is the bed roughness length (often approximated as D84/30 during hydraulically rough flows; Middleton and Southard, 1984). Moore et al. (2007) effectively reconstructed the 1929 Grand Banks tsunami from sediments deposited in Newfoundland, Canada.

Water depth and flow velocity (Fig. 23.2) have also been mathematically related (Woodruff et al., 2008) assuming near critical flow of a tidal bore traveling over near dry land at the point of complete suspension, so the average flow velocities within the bore are equal to its shallow water wave speed (i.e., $U = \sqrt{gh}$). Under such conditions water depth over the barrier (h_b) is approximated as shown:

$$\left\langle h_b \right\rangle = \left(\frac{{x_L}^2 {w_s}^2}{g}\right)^{\frac{1}{3}} \tag{23.9}$$

This model (Fig. 23.2) has been successfully applied to settings around the world, including modern and paleo-hurricane overwash deposits along the Caribbean (Woodruff et al., 2008), Atlantic (Brandon et al., 2014), South Pacific (Hong et al., 2018), and the Gulf of Mexico (Wallace and Anderson, 2010; Bregy et al., 2018), as well as tsunami deposits in Japan (Baranes et al., 2016).

The aforementioned particle trajectory models assume complete and unhindered settling following initial suspension, which is almost certainly an oversimplification of the process given the exclusion of turbulent resuspension common to highly energetic flows. They also generally assume that there is an abundance of sediment of varying grain sizes at the point of initial suspension, so the resulting deposit is not source limited. To account for non-uniform flow width associated with focused flow through low-lying regions of a coastal barrier, Baranes et al. (2016) added an additional term (f) to represent the ratio of flow width over the barrier relative to the inland width of inundation. A Froude number term (Fr_b) was also added to account for uncertainty in flow conditions and observations ranging between 0.8 and 1.5 along the backside of the barrier system (e.g., Holland et al., 1991; Donnelly et al., 2006). These additions resulted in the following relationship between settling velocity and flow depth:

$$w_S = \frac{f \quad Fr_b \quad \sqrt{g{h_b}^3}}{x_L} \tag{23.10}$$

Even with the additions in Eq. (23.10), results from any idealized trajectory model should always be viewed as approximate at best, yet still serving as a valuable constraint, particularly when providing a relative comparison of flood magnitudes for a sequence of deposits from a single site and assuming no major geomorphological changes have occurred over the period of comparison.

Equilibrium suspension

Jaffe and Gelfenbaum (2007) present an iterative equilibrium suspension model (TsuSedMod) based primarily on the fact that many tsunami deposits consist of a fining upward sequence (i.e., normal grading). During an approaching tsunami wave, sediment is stirred in suspension, with this sediment settling out of suspension as each tsunami wave slows (Fig. 23.3). From a normally graded tsunami deposit interval, this model can be used to calculate the necessary flow speed to suspend the observed sediment. Specifically, this model can be used if suspension (normal) grading is observed, where particular intervals within a tsunami deposit exhibit grain size distribution shifts toward finer deposits (Fig. 23.3). Additional basic assumptions for the applicability of this model include the following: 1) that sediment is transported in suspension, 2) a steady flow turbulence formulation is applicable to the phase close to the maximum speed of the tsunami, 3) significant sediment is available for suspension and subsequent deposition, 4) suspended sediment exists in the water column in equilibrium concentration profiles, 5) the resultant deposit is formed from clearing of equilibrium suspended sediment profiles, and 6) no erosion occurs during settling or the backwash process (Table 23.1).

The flow speed of the tsunami can be computed using the grain size distribution and thickness of a suspension-graded interval in the tsunami deposit, and assuming bottom roughness to link the flow conditions required for necessary equilibrium suspended sediment concentration profiles. To calculate equilibrium sediment concentration depth profiles resulting from the upward diffusion balance with the downward settling of grains, Jaffe and Gelfenbaum (2007) offer the following Rouse styled formulation:

$$C_i(z) = C_{r_i} e^{w_{s_i} \int_{z_{0total}}^{z} \frac{1}{K(z)}\, dz} \tag{23.11}$$

where $C_i(z)$ is the sediment concentration of a given size class i at elevation z above the bed, C_{r_i} is the reference concentration for given size class i, w_{s_i} is the settling velocity associated with size class i, z_{0total} is the bottom roughness parameter, and $K(z)$ is the eddy viscosity described as a function of the shear velocity, flow depth, and distance above the bed. In a refinement to the model, Jaffe et al. (2012) incorporated the ability to specify roughness coefficients using Manning's n, a higher roughness than used in Jaffe and Gelfenbaum (2007), which resulted in lower calculated tsunami flow speed.

To link the observed deposit grain sizes and amount of sediment in suspension for a specific suspension-graded section of a tsunami deposit, Jaffe et al. (2012) offer

a formulation, which iteratively adjusts the sediment source distribution and shear velocity. For a given grain size class, i,

$$\int_0^h C_i(z)dz = \int_{^zSGLbot}^{^zSGLtop} C_i(z)dz \tag{23.12}$$

where h is the tsunami flow depth, $C_i(z)$ is the sediment volume concentration of a given grain size class i at an elevation above the bed (z), ^zSGLbot is the bottom of a specific suspension-graded section of a tsunami deposit, and ^zSGLtop is the top of the same suspension-graded section.

Once the shear velocity (U_*) required to produce a specific suspension-graded interval of a tsunami deposit is determined, the flow speed profile for the tsunami, $U(z)$, can be determined using the following:

$$U(z) = \int_{z_0}^{z} \frac{U_*^2}{K(z)}dz \tag{23.13}$$

where z_0 is the roughness of the bottom, and $K(z)$ is the eddy viscosity.

TsuSedMod has been successfully applied to reconstruct modern tsunamis in Papua New Guinea (Jaffe and Gelfenbaum, 2007), Sumatra/Java (Spiske et al., 2010), Samoa (Jaffe et al., 2011), Japan (Jaffe et al., 2012), and paleotsunamis in Oregon (Witter et al., 2012) and Peru (Spiske et al., 2013).

Combined

Recent work has combined some previously discussed models, and they are briefly mentioned here but are beyond the scope of this chapter. A combined iterative model, TSUFLIND (Tang and Weiss, 2015) incorporates three previously discussed inverse models (Jaffe and Gelfenbaum, 2007; Moore et al., 2007; Soulsby et al., 2007). Important assumptions for this model are the following: 1) sediment transport and deposition during a tsunami are uniform in space and time, and 2) the deposit forms from horizontal convergence and suspension settling. Similar to previously discussed models, the tsunami deposit characteristics are extracted from field data to match sediment thicknesses and grain size distributions. TSUFLIND has been applied to the modern 2004 Indian Ocean Tsunami in India. For more details, the reader is referred to Tang and Weiss (2015).

TSUFLIND-EnKF (Tang et al., 2018) incorporates TSUFLIND as a forward model, an inversion method (EnKF), and the field data on which the inversion method is based. For more details, the reader is referred to Tang et al. (2018).

Experimental studies

Experimental, or laboratory flume, studies can be used to examine tsunami/storm wave propagation, sediment transport, and resulting deposition. As it is nearly impossible to observe these processes in real time during an event, these

experimental studies provide valuable insights. Additionally, as mentioned earlier, deposits often underconstrain some variables that can be associated with hydrodynamics, which require many inverse approaches to make simplifying assumptions (Johnson et al., 2016). Experimental studies can better constrain differences in bed versus suspended load sediment transport during tsunamis. These approaches have contributed to a better understanding of local sediment transport under extreme flow conditions (Yoshii et al., 2017). In general, these laboratory studies can provide important data concerning deposit source, grain size distributions, wave hydrodynamics, and the resultant deposits that can then quantitatively scale to natural tsunamis and storms. They are also useful in testing the preceding inverse approaches.

Experimental studies primarily use flumes of various dimensions and tsunamis of different wave characteristics to subsequently impact different sediment types, slopes, and morphologies (Takahashi et al., 2000; Yoshii et al., 2009; Yamaguchi and Sekiguchi, 2015; Johnson et al., 2016). The waves themselves are primarily created using water pumps and gates. Flow characteristics during the experiments are measured with devices such as cameras, wave gauges, laser flow meters, acoustic doppler velocimeters, ultrasonic transducers, and/or propeller flow meters. Turbidity can be measured using forward scattering sensors calibrated to suspended sediment concentration. Topography can be measured within the flume using laser displacement meters and cameras. Small sediment traps can be used to capture overflow. After an experimental run, the water is typically drained very slowly, leaving behind the resultant deposit. This deposit can then be photographed, scanned, measured, scraped, sliced, cored, and/or stored for further laboratory analyses.

Laboratory studies provide the opportunity to improve upon inversion models in that they can test the models without needing to wait for a destructive, infrequent natural event. These experimental studies have provided independent assessments of many aforementioned inverse numerical modeling studies. For example, Johnson et al. (2016, 2017) used experimental flume bores, which mimic the characteristics of tsunamis and storm surges. Johnson et al. (2016) applied the inverse model of Woodruff et al. (2008) to the deposits created in the experimental study. They discovered that at 95% confidence, the Woodruff et al. (2008) model predicts time-averaged flow depths for an event to about a factor of 2, and time-averaged flow velocities downstream to about a factor of 1.5. Johnson et al. (2017) determined that the median grain size within a deposit better predicted mean flow hydraulics as opposed to the 95^{th} percentile grain sizes. They also determined that transport distances longer than one to two advection length scales are needed for the grain size distribution in the deposit to be reasonably used to predict flow depths and velocities.

Laboratory studies also provide insight on tsunami deposit sedimentary structures as well as the validity of certain inverse model assumptions. Yoshii et al. (2017) showed that inverse grading was associated with depositional processes as opposed to the vertical distribution of grain sizes in the actual flow. They suggest that fine sand moved into the pore spaces between more coarse sand, while the coarse sand in the upper part of deposits implies that coarse sand was mobilized

during deposition. This process is known as kinetic sieving (dynamic sorting). Yoshii et al. (2017) also determined that sediment deposited near the tsunami inundation limit showed rapidly fining sediment of varying chemical compositions. Yoshii et al. (2018) determined that the inundation reached much further inland than sandy deposits. They observed the formation of an inversely graded deposit in a range of inland deposits, which they also attributed to kinetic sieving. Additionally, sediment behind the dunes became liquefied, which they hypothesize to be a sedimentary characteristic specific to earthquake-derived tsunamis.

Current challenges, potentialities and future directions

As discussed before, there is much that can be learned from experimental studies and inverse modeling approaches applied to tsunami and storm deposits, yet there remain a number of challenges. Primarily, testing all of these models with more global field observations and experimental studies remains of the utmost importance. While this has certainly been done to some degree (see preceding examples), this model validation can determine whether necessary assumptions are appropriate, in addition to how well the models can constrain processes such as flooding height, inundation, and flow speed. Another challenge with inverse models is quantifying uncertainty (Jaffe et al., 2016). Laboratory studies also face challenges, namely with scaling (Yoshii et al., 2017). For small-scale experiments, particle size and settling velocities are difficult to scale appropriately with that of the flow (Takahashi et al., 2000; Yoshii et al., 2009; Yamaguchi and Sekiguchi, 2015; Johnson et al., 2016). Experimental work has thus generally been moving toward larger scales, which often is cost and space prohibitive.

A limited understanding of the inundation and transport processes associated with tsunamis and storms presents challenges for applying these models discussed to paleo-events. While it is beyond the scope of this study, another major challenge in the field involves a coupling of inverse and forward approaches (Sugawara et al., 2014, 2015). These hybrid techniques, in addition to combined modeling approaches (e.g., Tang and Weiss, 2015; Tang et al., 2018), could yield tremendous insight for both modern and paleo-events, and they currently represent the cutting edge for this field.

Conclusions

Field-based surveying, experimental studies, and inverse numerical models should be viewed as a continuum of investigations, which can greatly aid in understanding tsunami and storm impacts. This chapter outlines typical field survey sampling considerations, noting that no two events are exactly alike and require an adaptable approach in terms of sampling and study. Inverse numerical models can be applied to these deposits to better constrain event parameters such as flooding height, inundation, and flow speed. Experimental models use laboratory observations in flumes

to examine flow characteristics and associated deposits and can be compared with field observations and inverse approaches. However, in essence, inverse and experimental approaches are idealistic flooding scenarios and should be regarded as overly simplistic views of the tsunami/storm flooding process. Both require a number of assumptions to be applicable to naturally occurring events. Realistically, both models and experimental work should be viewed as a method for generally constraining tsunami/storm characteristics rather than arriving at an exact solution. Since the most destructive tsunami and storm events are rare, and it is often challenging or impossible to directly measure certain characteristics, the insight gleaned from the combination of field, modeling, and experimental studies still offers the best opportunity for constraining flow and sediment transport conditions. Therefore, their application in addition to the future directions outlined before should continue to be important considerations in tsunami and storm research.

Acknowledgments

The authors would like to thank helpful reviews from Bruce Jaffe and an anonymous reviewer, which significantly improved this chapter. This material is based upon work supported by the National Science Foundation under award no. 1630090 to Woodruff.

References

Baranes, H.E., Woodruff, J.D., Wallace, D.J., Kanamaru, K., Cook, T.L., 2016. Sedimentological records of the CE 1707 Hōei Nankai Trough tsunami in the Bungo Channel, southwestern Japan. Natural Hazards 84, 1185−1205. https://doi.org/10.1007/s11069-016-2498-3.

Brandon, C.M., Woodruff, J.D., Donnelly, J.P., Sullivan, R.M., 2014. How unique was Hurricane Sandy? Sedimentary reconstructions of extreme flooding from New York Harbor. Scientific Reports 4, 7366. https://doi.org/10.1038/srep07366.

Bregy, J.C., Wallace, D.J., Minzoni, R.T., Cruz, V.J., 2018. 2500-year paleotempestological record of intense storms for the Northern Gulf of Mexico, United States. Marine Geology 396, 26−42. https://doi.org/10.1016/j.margeo.2017.09.009.

Bricker-Urso, S., Nixon, S.W., Cochran, J.K., Hirschberg, D.J., Hunt, C., 1989. Accretion rates and sediment accumulation in Rhode Island salt marshes. Estuaries 12, 300−317. https://doi.org/10.2307/1351908.

Brugam, R.B., 1978. Human disturbance and the historical development of Linsley Pond. Ecology 59, 19−36. https://doi.org/10.2307/1936629.

Coleman, P.J., 1968. Tsunamis as geological agents. Journal of the Geological Society of Australia 15 (2), 267−273. https://doi.org/10.1080/00167616808728698.

DeLaune, R.D., Patrick Jr., W.H., Buresh, R.J., 1978. Sedimentation rates determined by 137Cs dating in a rapidly accreting salt marsh. Nature 275, 532−533. https://doi.org/10.1038/275532a0.

Donnelly, C., Kraus, N.C., Larson, M., 2006. State of knowledge on measurement and modeling of coastal overwash. Journal of Coastal Research 22, 965−991. https://doi.org/10.2112/04-0431.1.

Faure, G., 1986. Principles of Isotope Geology. Wiley, New York, 589 pp.
Ferguson, R.I., Church, M., 2004. A simple universal equation for grain settling velocity. Journal of Sedimentary Research 74, 933–937. https://doi.org/10.1306/051204740933.
Hayes, M.O., 1967. Hurricanes as geological agents: case studies of Hurricanes Carla, 1961, and Cindy, 1963. Bureau of Economic Geology. Report of Investigation 61. https://doi.org/10.23867/RI0061D.
Holland, T.K., Holman, R.A., Sallenger Jr., A.H., 1991. Estimation of overwash bore velocities using video techniques. In: Kraus, N.C., Gingerich, K.J., Kriebel, D.L. (Eds.), Coastal Sediments 1991. American Society of Civil Engineers, Washington D.C., pp. 489–497.
Hong, I., Pilarczyk, J.E., Horton, B.P., Fritz, H.M., Kosciuch, T., Wallace, D.J., Dike, C., Rarai, A., Harrison, M.J., Jockley, F.R., 2018. Sedimentological characteristics of the 2015 Tropical Cyclone Pam overwash sediments from Vanuatu, South Pacific. Marine Geology 396, 205–214. https://doi.org/10.1016/j.margeo.2017.05.011.
International Tsunami Survey Team (ITST), 2014. Post-tsunami Survey Field Guide. IOC Manuals and Guides No. 37, 2nd ed. UNESCO, Paris. http://unesdoc.unesco.org/images/0022/002294/229456E.pdf. last access: 10.03.2020.
Jaffe, B.E., Buckley, M.L., Richmond, B.M., Strotz, L., Etienne, S., Clark, K., Gelfenbaum, G., 2011. Flow speed estimated by inverse modeling of sandy sediment deposited by the 29 September 2009 tsunami near Satitoa, east Upolu, Samoa. Earth-Science Reviews 107, 23–37. https://doi.org/10.1016/j.earscirev.2011.03.009.
Jaffe, B.E., Gelfenbaum, G., 2007. A simple model for calculating tsunami flow speed from tsunami deposits. Sedimentary Geology 200, 347–361. https://doi.org/10.1016/j.sedgeo.2007.01.013.
Jaffe, B.E., Goto, K., Sugawara, D., Richmond, B., Fujino, S., Nishimura, Y., 2012. Flow speed estimated by inverse modeling of sandy tsunami deposits: results from the 11 March 2011 tsunami on the coastal plain near the Sendai Airport, Honshu, Japan. Sedimentary Geology 282, 90–109. https://doi.org/10.1016/j.sedgeo.2012.09.002.
Jaffe, B., Goto, K., Sugawara, D., Gelfenbaum, G., La Selle, S., 2016. Uncertainty in tsunami sediment transport modeling. Journal of Disaster Research 11, 647–661. https://doi.org/10.20965/jdr.2016.p0647.
Johnson, J.P.L., Delbecq, K., Kim, W., Mohrig, D., 2016. Experimental tsunami deposits: linking hydrodynamics to sediment entrainment, advection lengths and downstream fining. Geomorphology 253, 478–490. https://doi.org/10.1016/j.geomorph.2015.11.004.
Johnson, J.P.L., Delbecq, K., Kim, W., 2017. Predicting paleohydraulics from storm surge and tsunami deposits: using experiments to improve inverse model accuracy. Journal of Geophysical Research: Earth Surface 122, 760–781. https://doi.org/10.1002/2015JF003816.
Kahn, J.H., Roberts, H.H., 1982. Variations in storm response along a microtidal transgressive barrier- island arc. Sedimentary Geology 33, 129–146. https://doi.org/10.1016/0037-0738(82)90046-x.
Kon'no, E., 1961. Geological observation of the Sanriku coastal region damaged by the tsunami due to the Chile earthquake in 1960. Contributions from the Institute of Geology and Paleontology, Tohoku University 52, 1–45 (in Japanese with English abstract).
La Selle, S.M., Lunghino, B.D., Jaffe, B.E., Gelfenbaum, G., Costa, P.J.M., 2017. Hurricane Sandy Washover Deposits on Fire Island. Open-File Report 2017–1014. U.S. Geological Survey, New York. https://doi.org/10.3133/ofr20171014, 30 pp.
Libby, W.F., 1955. Radiocarbon Dating. University of Chicago Press, Chicago.

Libby, W.F., Anderson, E.C., Arnold, J.R., 1949. Age determination by radiocarbon content: world-wide assay of natural radiocarbon. Science 109, 227–228. https://doi.org/10.1126/science.109.2827.227.

Makino, K., 1968. The Meiwa Tsunami at Yaeyama. Ishigaki. (in Japanese).

McCaffrey, R.J., Thomson, J., 1980. A record of the accumulation of sediment and trace metals in a Connecticut salt marsh. In: Saltzman, B. (Ed.), Estuarine Physics and Chemistry: Studies in Long Island Sound. Academic Press, New York, pp. 165–236.

Middleton, G.V., Southard, J.B., 1984. Mechanics of Sediment Movement, 2nd ed. SEPM, Tulsa, OK.

Moore, A.L., McAdoo, B.G., Ruffman, A., 2007. Landward fining from multiple sources in a sand sheet deposited by the 1929 Grand Banks tsunami, Newfoundland. Sedimentary Geology 200, 336–346. https://doi.org/10.1016/j.sedgeo.2007.01.012.

Morton, R.A., 1979. Subaerial storm deposits formed on barrier flats by wind-driven currents. Sedimentary Geology 24, 105–122. https://doi.org/10.1016/0037-0738(79)90031-9.

Morton, R.A., Gelfenbaum, G., Jaffe, B.E., 2007. Physical criteria for distinguishing sandy tsunami and storm deposits using modern examples. Sedimentary Geology 200, 184–207. https://doi.org/10.1016/j.sedgeo.2007.01.003.

Nummedal, D., Penland, S., Gerdes, R., Schramm, W., Kahn, J., Roberts, H., 1980. Geologic response to hurricane impact on low-profile Gulf Coast Barriers. Transactions: Gulf Coast Association of Geological Societies 30, 183–195.

Page, M.J., Trustrum, N.A., Orpin, A.R., Carter, L., Gomez, B., Cochran, U.A., Mildenhall, D.C., Rogers, K.M., Brackley, H.L., Palmer, A.S., Northcote, L., 2010. Storm frequency and magnitude in response to Holocene climate variability, Lake Tutira, North-Eastern New Zealand. Marine Geology 270, 30–44. https://doi.org/10.1016/j.margeo.2009.10.019.

Piatanesi, A., Tinti, S., Gavagni, I., 1996. The slip distribution of the 1992 Nicaragua earthquake from tsunami run-up data. Geophysical Research Letters 23, 37–40. https://doi.org/10.1029/95gl03606.

Pilarczyk, J.E., Dura, T., Horton, B.P., Engelhart, S.E., Kemp, A.C., Sawai, Y., 2014. Microfossils from coastal environments as indicators of paleo-earthquakes, tsunamis and storms. Palaeogeography, Palaeoclimatology, Palaeoecology 413, 144–157. https://doi.org/10.1016/j.palaeo.2014.06.033.

Rich, P.H., 1970. Post-settlement influences upon a southern Michigan marl lake. Michigan Botanist 9, 3–9.

Satake, K., Bourgeois, J., Abe, K., Abe, K., Tsuji, Y., Imamura, F., Iio, Y., Katao, H., Noguera, E., Estrada, F., 1993. Tsunami field survey of the 1992 Nicaragua earthquake. Eos Transactions American Geophysical Union 74 (145), 156–157. https://doi.org/10.1029/93eo00271.

Shepard, F.P., Macdonald, G.A., Cox, D.C., 1950. The Tsunami of April 1, 1946. Bulletin of the Scripps Institution of Oceanography 5, 391–528.

Smith, D.E., Foster, I.D.L., Long, D., Shi, S., 2007. Reconstructing the pattern and depth of flow onshore in a palaeotsunami from associated deposits. Sedimentary Geology 200, 362–371. https://doi.org/10.1016/j.sedgeo.2007.01.014.

Soulsby, R., 1997. Dynamics of Marine Sand. Thomas Telford, London.

Soulsby, R.L., Smith, D.E., Ruffman, A., 2007. Reconstructing tsunami run-up from sedimentary characteristics – a simple mathematical model. Coastal Sediments '07, 1075–1088.

Spiske, M., Weiss, R., Bahlburg, H., Roskosch, J., Amijaya, H., 2010. The TsuSedMod inversion model applied to the deposits of the 2004 Sumatra and 2006 Java tsunami and implications for estimating flow parameters of paleo-tsunami. Sedimentary Geology 224, 29–37. https://doi.org/10.1016/j.sedgeo.2009.12.005.

Spiske, M., Piepenbreier, J., Benavente, C., Kunz, A., Bahlburg, H., Steffahn, J., 2013. Historical tsunami deposits in Peru: sedimentology, inverse modeling and optically stimulated luminescence dating. Quaternary International 305, 31–44. https://doi.org/10.1016/j.quaint.2013.02.010.

Stone, G.W., Wang, P., 1999. The importance of cyclogenesis on the short-term evolution of Gulf Coast barriers. Transactions: Gulf Coast Association of Geological Societies 49, 478–487.

Sugawara, D., Goto, K., Jaffe, B.E., 2014. Numerical models of tsunami sediment transport – current understanding and future directions. Marine Geology 352, 295–320. https://doi.org/10.1016/j.margeo.2014.02.007.

Sugawara, D., Jaffe, B., Goto, K., Gelfenbaum, G., La Selle, S., 2015. Exploring hybrid modeling of tsunami flow and deposit characteristics. Coastal Sediments '15. https://doi.org/10.1142/9789814689977_0185.

Switzer, A.D., Jones, B.G., 2008. Large-scale washover sedimentation in a freshwater lagoon from the southeast Australian coast: sea-level change, tsunami or exceptionally large storm? The Holocene 18, 787–803. https://doi.org/10.1177/0959683608089214.

Synolakis, C., Okal, E., 2005. 1992–2002: Perspective on a decade of post-tsunami surveys. In: Satake, K. (Ed.), Tsunamis – Case Studies and Recent Developments. Springer, Dordrecht, pp. 1–29. https://doi.org/10.1007/1-4020-3331-1_1.

Syvitski, J.P.M., Asprey, K.W., Clattenburg, D.A., 1991. Principles, design, and calibration of settling tubes. In: Syvitski, J.P.M. (Ed.), Principles, Methods, and Application of Particle Size Analysis. Cambridge University Press, Cambridge, pp. 45–63. https://doi.org/10.1017/CBO9780511626142.007.

Takahashi, T., Shuto, N., Imamura, F., Asai, D., 2000. Modeling sediment transport due to tsunamis with exchange rate between bed load layer and suspended load layer. In: Proceedings of the 27th International Conference on Coastal Engineering, pp. 1508–1519. https://doi.org/10.1061/40549(276)117.

Tang, H., Weiss, R., 2015. A model for tsunami flow inversion from deposits (TSUFLIND). Marine Geology 370, 55–62. https://doi.org/10.1016/j.margeo.2015.10.011.

Tang, H., Wang, J., Weiss, R., Xiao, H., 2018. TSUFLIND-EnKF: inversion of tsunami flow depth and flow speed from deposits with quantified uncertainties. Marine Geology 396, 16–25. https://doi.org/10.1016/j.margeo.2016.11.009.

Wallace, D.J., Anderson, J.B., 2010. Evidence of similar probability of intense hurricane strikes for the Gulf of Mexico over the late Holocene. Geology 38, 511–514. https://doi.org/10.1130/g30729.1.

Wilson, R., Wood, N., Kong, L., Shulters, M., Richards, K., Dunbar, P., Tamura, G., Young, E., 2015. A protocol for coordinating post-tsunami field reconnaissance efforts in the USA. Natural Hazards 75, 2153–2165. https://doi.org/10.1007/s11069-014-1418-7.

Witter, R.C., Jaffe, B.E., Zhang, Y., Priest, G., 2012. Reconstructing hydrodynamic flow parameters of the 1700 tsunami at Cannon Beach, Oregon, USA. Natural Hazards 63, 223–240. https://doi.org/10.1007/s11069-011-9912-7.

Woodruff, J.D., Donnelly, J.P., Mohrig, D., Geyer, W.R., 2008. Reconstructing relative flooding intensities responsible for hurricane-induced deposits from Laguna Playa Grande, Vieques, Puerto Rico. Geology 36, 391–394. https://doi.org/10.1130/g24731a.1.

Yamaguchi, N., Sekiguchi, T., 2015. Effects of tsunami magnitude and terrestrial topography on sedimentary processes and distribution of tsunami deposits in flume experiments. Sedimentary Geology 328, 115−121. https://doi.org/10.1016/j.sedgeo.2015.08.008.

Yoshii, T., Ikeno, M., Matsuyama, M., 2009. Experimental study of sediment transport caused by tsunami. In: Proceedings of Coastal Dynamics. https://doi.org/10.1142/9789814282475_0035.

Yoshii, T., Tanaka, S., Matsuyama, M., 2018. Tsunami inundation, sediment transport, and deposition process of tsunami deposits on coastal lowland inferred from the Tsunami Sand Transport Laboratory Experiment (TSTLE). Marine Geology 400, 107−118. https://doi.org/10.1016/j.margeo.2018.03.007.

Yoshii, T., Tanaka, S., Matsuyama, M., 2017. Tsunami deposits in a super-large wave flume. Marine Geology 391, 98−107. https://doi.org/10.1016/j.margeo.2017.07.020.